Long-range transatlantic transport of microorganisms in clouds of African desert dust: a study of atmospheric microbiology, chemistry, and the influence of desert dust on surface water microbial ecology aboard the R/V *JOIDES Resolution*, IODP Expedition 336, 16 September–16 November 2011[1]

Dale W. Griffin[2]

Chapter contents

Project summary

Atmospheric samples were collected daily while in transit and on site from 19 September to 11 November 2011 (54 sample days). This report summarizes data collected from 19 September to 1 November (44 sample days) due to incubation period constraints.

Standard geochemical and molecular microbiology techniques will be used to identify microorganisms and inorganic constituents present in the atmosphere during both clear and desert dust conditions. Additionally, this project will investigate the influence of desert dust deposition on surface water microbial ecology using epifluorescent direct count, universal 16S, and *Vibrio* spp. specific quantitative polymerase chain reaction assays. Recently, African desert dust was found to increase the numbers of cultivable *Vibrio* spp. in Gulf of Mexico surface waters. These surface water and atmospheric data will provide insight into the numbers (16S and 18S quantitative polymerase chain reaction [qPCR] and cultivable) and diversity (16S and 18S sequences from qPCR and culture assays) of microorganisms transported in clouds of desert dust across the Atlantic to the Caribbean and Americas, the types of inorganic constituents found associated with dust events, and the influence of surface water dust deposition on microbial direct counts and the presence of total (qPCR) and cultivable *Vibrio* spp. The research sites for Integrated Ocean Drilling Program (IODP) Expedition 336 are within the transatlantic desert dust corridor and provide a unique opportunity to advance our understanding in a field of research that is not well understood. Dust particulates collected during this mission will be used to conduct experiments for a previously funded Centers for Disease Control and Prevention (CDC) grant entitled "Climate-change based predictive modeling of rising *Vibrio* illness in the U.S. 2011–2012" (Principal Investigator: Dr. Erin K. Lipp, University of Georgia at Athens).

Overview

The current estimate of the quantity of desert dust that moves through Earth's atmosphere each year ranges from 0.5 to 5.0 metric

tons (Perkins, 2001). A majority (50%–75%) of this quantity is believed to originate from the Sahara and Sahel Deserts in North Africa (Moulin et al., 1997; Perry et al., 1997; Goudie and Middleton, 2001; Prospero and Lamb, 2003). In general, high-energy storm activities over deserts and other arid regions can mobilize significant quantities of soil into the atmosphere (Gillies et al., 1996; Qian et al., 2002). Desert soils originating from the vast desert landscape of North Africa can impact air quality in the Middle East, Europe, the Caribbean, and the Americas.

Source regions of dust in the Sahara include the Bodele depression and a region covering western Mali, southern Algeria, and eastern Mauritania (Goudie and Middleton, 2001; Middleton and Goudie, 2001). Lake Chad, located southwest of the Bodele depression, is a significant source of dust in this region because of the exposed and dry lake bed. In 1963, Lake Chad had a surface area of 25,000 km² that was reduced to ~1,350 km² by 1997 as a result of the current North African drought and anthropogenic activity (Coe and Foley, 2001). Although anthropogenic activities (deforestation and desertification) in the Sahara and Sahel Deserts are also believed to influence dust transport, analyses of data collected between 1980 and 1997 demonstrated year-to-year variation in the overall size of the desert regions but no longer term changes (Tucker and Nicholson, 1999).

North African annual rainfall rates are influenced by atmospheric systems such as the North Atlantic Oscillation (NAO) and the El Niño Southern Oscillation (ENSO). The NAO has been in a predominantly positive (northerly) phase over the North Atlantic Ocean since the late 1960s, which has corresponded with an overall decrease in rainfall over North Africa (Moulin et al., 1997). It has also corresponded with a general increase in the amount of desert soil being delivered to the Caribbean and Americas (Prospero, 1999). Compared to the overall trend in dust deposition noted in the Caribbean, some of the highest deposition rates have corresponded with major ENSO events (Prospero and Nees, 1986; Prospero and Lamb, 2003; Shinn et al., 2003). Although dust transport out of North Africa may move north into the North Atlantic and Europe and northwest into the Middle East at various times of the year, the most consistent transport is across the Atlantic to the Caribbean and Americas (Perry et al., 1997). Transatlantic dust transport generally occurs between latitudes 15° and 25°N (Graham and Duce, 1979). Latitudinal Saharan/Sahel dust transport across the Atlantic is influenced by seasonal Hadley Cell shifts (Isard and Gage, 2001). In the Northern Hemisphere summer (June–October), dust transport is to the mid- to

northern Caribbean and North America, and during the winter (November–May) transport is to the mid- to southern Caribbean and South America (Graham and Duce, 1979). On 7 January 1999, a "blood rain" deposited an estimated 47 metric tons of dust on the Island of Tenerife (Criado and Dorta, 2003). It has been estimated that 40 million metric tons of African dust is deposited in the Amazon Basin each year (Koren et al., 2006).

Negative impacts of dust movement include transport of toxins (i.e., agricultural and industrial emissions), harmful algal blooms, and long-range transport of pathogenic microorganisms (O'Malley and McCurdy, 1990; Barrie et al., 1992; O'Hara et al., 2000; Weir et al., 2004; Griffin et al., 2001, 2006; Lenes et al., 2001; Walsh and Steidinger, 2001; Garrison et al., 2006; Griffin, 2007). Dust clouds may contain high concentrations of organics composed of plant detritus and microorganisms (Griffin et al., 2002; Jaenicke, 2005; Griffin, 2007) and may pick up additional biological loads (fungal spores, bacteria, viruses, pollen, etc.) as the clouds move through and sandblast downwind terrestrial environments or pass over aquatic environments, where microbial-laden fine-sized aquatic sprays adhere to dust particles (Grini and Zender, 2004). All of these dust cloud constituents may negatively influence human health in downwind environments, with the greatest risk factors being frequency of exposure, concentration of and composition of particulates, and immunological status (Griffin, 2007). Of particular interest is the transport of dust-borne pathogenic microorganisms that may impact human and ecosystem health.

Desert dust research has demonstrated the ability of diverse groups of bacteria and fungi to survive long-range atmospheric transport in clouds of desert dust (Griffin, 2007). In dust source regions, a single gram of topsoil may contain 10^9 and 10^6 bacteria cells and fungal cells and spores, respectively, in addition to communities of protozoa and viruses (Whitman et al., 1998; Tate, 2000). In regard to both bacteria and fungi, the extent of diversity is probably much greater than previously reported given that the majority of published papers on the topic only report culture-based approaches and it is known that the given number of colonies isolated from any sample type typically represent <1% of what is actually present (Whitman et al., 1998).

It is obvious from a review of the scientific literature that dust storms can transport constituents such as toxic compounds and microorganisms that may negatively impact human and ecosystem health. What is surprising is that few (<40) studies to date have been conducted on this topic, and many of those are significantly dated. There is a clear need for studies

geared at addressing this topic, and the field is wide open for many varied scientific disciplines (e.g., microbiology, toxicology, epidemiology, etc.).

Objectives

The overall objective of this study is to evaluate the biological and chemical constituents of African desert dust impacting IODP Expedition 336 prospectus Sites NP-1 through NP-4, located in the mid-Atlantic, as follows:

- Use a laser particle counter, the Navy Aerosol Analysis and Prediction System (NAAPS) (Douglas Westphal, Naval Research Laboratory, Monterey CA), and Moderate Resolution Imaging Spectroradiometer (MODIS) satellite imagery to monitor dust movement to and across Expedition 336 research sites.

- Use low-volume membrane filtration, high-volume membrane filtration, and a high-volume liquid impinger to collect samples daily for microbiology and chemical analyses.

- Use established culture and molecular assays to identify microorganisms (colony counts and DNA sequence data) in atmospheric samples. These assays will include standard culture-based assays, as published (Griffin et al., 2001), in addition to standard and qPCR sequencing assays, to identify organisms that are present in both atmospheric and surface water samples.

- Use epifluorescence microscopy to obtain the total number of bacteria and viruses present (direct count assay) in surface water samples.

- Use direct count assay data, *Vibrio* spp.–specific qPCR, and *Vibrio* spp. cultures to determine the influence of aerosol deposition in surface waters.

- Identify inorganic desert dust constituents from particulates collected with the high-volume membrane filtration unit using wavelength dispersive X-ray fluorescence.

- Screen all liquid impinger samples for the presence or absence of bird and human influenza and foot and mouth disease viruses (a Taiwanese scientist just reported an increase in airborne influenza viruses during an Asian dust event that impacted air quality in Taiwan; Chen et al., 2010).

Methods

All described data were logged using a laboratory notebook and Microsoft Excel spreadsheet; all equipment was mounted on top of the bridge on the port side of the ship to minimize potential ship-borne contamination of the samples.

Atmospheric and ship parameters

Each morning when the R/V *JOIDES Resolution* was on site, atmospheric parameters including temperature, barometric pressure, humidity, wind speed, and wind direction were logged using a Kessler 4500 anemometer and ship compass. When the *JOIDES Resolution* was under way, measurements were taken at the end of the low-volume filtration A sample period. Between ~1100 and 1300 h (local time; Universal Time Coordinated [UTC] – 3 h) each day, ultraviolet-C (UVC)-254 and ultraviolet (UV)-40 measurements were taken using UV meters. Ship data were taken each morning and while under way at the end of each sample period and include GPS latitude and longitude, ship heading, and ship speed.

Particle count data

A ParticleScan Pro was used to collect particle count data every 10 min, daily. These data were logged into an Excel spreadsheet using a laptop running Microsoft Windows. Daily spreadsheets of these data were saved using the following naming convention: (month/day/year)iodp336. These data were used to determine daily and per sample period aerosol loads.

Low-volume membrane filtration samples

One short-term and one long-term low-volume sample were collected daily. Short-term samples were collected over ~4 h and long-term samples were collected over ~12 h using a portable apparatus as previously described (flow rate = ~1.75–3.5 L/min, as logged). These samples were plated on R2A media and incubated at room temperature in the dark. Bacterial and fungal colony forming unit (CFU) growth was monitored over a 10 day period and logged. CFUs were picked and stored in cryogenic storage for shore-based sequence identification. A maximum of 5 CFUs were picked from those plates where the CFUs appear to be identical in morphology and pigmentation.

High-volume membrane filtration samples

High-volume membrane filtration samples were collected over a 24 h period and started daily at ~0700 h. The high-volume membrane filtration unit was a Staplex TF1A filtration unit, and TFAGF41 glass fiber filters were employed for this study. Each filter was weighed daily, and the filter housing was assembled with the filter in place, wrapped in aluminum foil, and autoclaved prior to use. The unit flow rate is 20 ft^3/min. After filtration, the filter was stored in a labeled zip-top bag at –80°C.

Liquid impinger samples

Liquid impinger samples were collected over a 4 h period daily between 0500 and 1200 h (time is Eastern Standard Time [EST] unless otherwise stated; up to 6 November UTC = EST + 5 h, starting 6 November UTC = EST + 4 h). For onboard analyses, 100 µL aliquots were spread-plate with R2A and TCBS agar. R2A media was used to determine cultivable bacteria and fungi, and TCBS agar was used to determine cultivable *Vibrio* spp. Plates were incubated at room temperature in the dark and enumerated at 5 and 10 days. After spread-plating was completed, the samples were stored at –80°C. These samples will be screened for bacteria and fungi using universal qPCR analyses postexpedition.

Surface water samples

Surface water grabs (~45–50 mL) were collected daily between 1045 and 1200 h from a port/bow location (under the bridge) at a maximum depth of ~0.25 m using a 50 mL tube and weight attached to a string. Salinity, temperature, and pH were recorded using a thermometer, handheld pH meter, and refractometer. Two 100 µL samples were used for spread-plate *Vibrio* analyses. Samples were incubated for 10 days at room temperature in the dark, and CFUs were enumerated at 5 and 10 days. CFU pigmentation (yellow or green) was recorded for each colony. All colonies were picked and subcultured in ~500 µL of TSB media. These isolates were incubated for a minimum of 3 days at room temperature, at which time ~200 µL of glycerol was added to each tube. The tubes were then vortexed and stored at –80°C for postexpedition 16S sequence identification. For each sample, two 1 mL subsamples were centrifuged for 20 min at 14,500 rotations per minute (rpm); after centrifugation, the supernatant was removed and discarded using a micropipette. These samples were stored at –80°C for postexpedition qPCR analyses for total bacteria and *Vibrio* spp. Two 10 mL subsamples were used for bacteria and viruslike particle direct counts. The protocol used for these assays follows Griffin et al. (2001). The remaining aliquot of surface water for each sample date was stored at –80°C for postexpedition cataloging.

Results

The period covered for this report is 19 September–1 November 2011. Pearson's product-moment correlation (SPSS) was utilized for statistical analyses. All data were normally distributed according to the Kolmogorov-Smirnov test.

Ship and atmospheric data

Ship heading (direction of bow) and cruising speed were recorded daily. During the period 19 September–1 November, the *JOIDES Resolution* was on site from 21 to 28 September and 2 October to 1 November. During these two periods, the bow was generally into the wind and pointing east. On 19 and 20 September and 29 September–1 October the *JOIDES Resolution* was in transit (avoiding the peripheral path effects of Tropical Storm Philippe), and the heading recordings taken each morning were 7°, 13°, 60°, 145°, and 275°, respectively. The only days where the orientation of the bow was far removed from east was 27 September (200°), 28 September (360°), and 11 and 12 October (185°). Atmospheric data comprising humidity, barometric pressure, temperature, wind speed, and wind direction were recorded each morning to coincide with the morning sample start times, and UV-340 and UVC-254 were recorded at the end of the low-volume A sample period (~1000–1100 h in most cases). Humidity ranged from 65.8% to 84.3% (average = 74.5%), barometric pressure ranged from 29.9 to 30.1 mm Hg (average = 30.0 mm Hg), temperature ranged from 25.4° to 30.1°C (average = 26.6°C), wind speed ranged from 0.7 to 13.5 m/s (average = 5.5 m/s; Fig. F1), UV-340 ranged from 33 to 316 µW/cm² (average = 161.2 µW/cm²; instrument set range = 2000–19990 × 10), and UVC-254 ranged from 0.037 to 0.439 mW/cm² (average = 0.296 mW/cm²; instrument set range = 1.999).

Particle counts

Particle counts were taken daily at a frequency of once every 10 min, with the exception of 27–29 September, when a faulty pump battery interfered with the AC adapter current flow. On 28 September, particle counts were obtained for the low-volume A sample period. For the purposes of charting, 27 September estimates were obtained by averaging the 26 and 30 September counts, the 28 September counts (except the low-volume A sample period) were obtained by averaging the acquired 27 September estimate and the 30 September counts, and the 29 September counts were obtained by averaging the acquired 28 September estimate and the 30 September counts. Particle counts for the sample periods were as follows: low-volume A samples ranged from 1.64×10^6 to 9.63×10^7 (average = 3.54×10^7) particles/L³; low-volume B samples ranged from 2.63×10^6 to 7.30×10^7 (average = 3.02×10^7) particles/L³; liquid impinger samples ranged from 5.20×10^4 to 1.31×10^8 (average = 3.92×10^7) particles/L³; and high-volume samples ranged from 1.82×10^6 to 5.17×10^7 (average = 2.34×10^7) particles/L³ (Fig. F2). In all

cases, the highest concentrations of particles fell within the >0.3–0.5 µm size range (representing ~80%–90% of the total particle count).

High-volume membrane filtration samples

High-volume membrane filtration was used to collect airborne particulates each day, with the exception of the 29 October sample, when the pump brushes were serviced. The flow rate for each sample was 20 ft³/min. Samples were started daily between 0645 and 1215 h and were stopped the following morning between 0500 and 0715 h. Visual results are illustrated in Figures F3 and F4. These samples will be used for universal 16S and 18S rRNA qPCR to obtain total bacterial and fungal counts and analyses for particulate chemical composition. Filters were stored in cryogenic storage for shore-based analyses. Each filter was photographed by IODP-United States Implementing Organization (USIO) Senior Imaging Specialist Bill Crawford, and associated data were provided to IODP-USIO Applications Developer Algie Morgan for IODP cataloging.

Low-volume membrane filtration samples

Two low-volume samples were collected daily. Low-volume A was started in the morning and collected over a 4–6 h period, with flow rates ranging from 1.75 to 9.4 L/min. Low-volume B was a longer period sample that was collected throughout the day at a flow rate ranging from 3.5 to 9.4 L/min. Low-volume A bacterial and fungal CFUs ranged from 0 to 6.34 CFU/m³ and 0 to 4.87 CFU/m³ of air, respectively. The total CFU range was the same because bacteria and fungus were not detected simultaneously in any of these samples. For this sample set, bacteria and fungus were detected in 6 and 4 of the 44 samples, respectively. Low-volume B bacterial and fungal CFUs ranged from 0 to 0.55 CFU/m³ and 0 to 4.76 CFU/m³ of air, respectively. Total CFUs (bacteria and fungus) ranged from 0 to 4.76 CFU/m³ of air (Fig. F5). Total CFU and particulate counts were statistically correlated ($r = 0.360$, $P = .017$). For this sample set, bacteria and fungus were detected in 4 and 16 of the 44 samples, respectively. In total, they were detected in 18 of the 44 samples. For both low-volume samples, isolates were picked, cultured in TSB media, and stored in cryogenic storage for shore-based 16S and 18S sequence-based identification.

Liquid impinger samples

Liquid impinger samples were collected daily between 0500 and 1430 h over a period of 1–4 h. Sample volumes ranged from ~18 to 78 m⁻³ of air. CFU, isolate identification, 16S and 18S qPCR, and signifi-cance to atmospheric particle counts will be evaluated on shore.

Surface water samples

Surface water samples were collected daily between 1110 and 1425 h. For the sample set, temperature ranged from 23.5° to 29.5°C (average = 27.1°C), pH ranged from 8.4 to 8.5 (average = 8.4), and refractometer salinity measurements ranged from 37.5 to 40 (average = 39.4). Bacterial and viruslike direct counts are illustrated in Figure F6. Bacterial counts ranged from 2.85×10^5 to 4.82×10^5 (average = 3.78 × 10⁵) counts/mL. Viruslike particle direct counts ranged from 1.45×10^6 to 3.77×10^6 (average = 2.50 × 10⁶) counts/mL. Bacterial and viruslike particle direct counts were significantly correlated ($r = 0.384$, $P = .010$). Bacterial counts were also significantly correlated with the high-volume time period (daily) atmospheric particle counts ($r = 0.383$, $P = .010$) (Fig. F7). Viruslike particle direct counts were not significantly correlated with the high-volume time period atmospheric particle counts. Culturable *Vibrio* spp. were detected on 28 September and 8 and 13 October at concentrations of 1.25×10^4, 5.0×10^2, and 5.0×10^2 CFU/100 mL, respectively. The *Vibrio* colonies were picked, cultured in TSB media, and stored cryogenically for shore-based 16S identification. Daily aliquots of pelleted cells and of noncentrifuged surface water samples were stored in cryogenic storage for shore-based 16S universal and *Vibrio* spp. qPCR. These data will be used to test association hypothesis.

Conclusions

These data indicate that atmospheric particulate matter moving over the Atlantic from Europe and Africa carries culturable microorganisms and that CFU concentrations in these air masses correlate with particulate concentrations. Further, these data demonstrate a "fertilization effect," where surface water prokaryote concentrations relate to near-surface atmospheric particulate concentrations. As can be seen in Figures F3 and F4, there were numerous episodes of African dust presence in the near-surface atmosphere over the period of this study. The dark and light orange filters in these two figures are similar in color to desert surface soils of the Sahara and Sahel and to longer period samples that were collected aboard the *JOIDES Resolution* during Ocean Drilling Program Leg 209, when African dust was present in the atmosphere. These samples will be evaluated for chemical composition at shore-based facilities. A colleague at the University of La Laguna in the Canary Islands notified me of dust episodes impacting air quality there on 30 September and 13 October and

forecasted the presence of dust at Expedition 336 drill sites on 1 and 15 October, respectively. Following the dust episode of 1 October, dust that fell onto the roof over the bridge of the *JOIDES Resolution* was present at concentrations that were clearly visible, and the dust imaged (in a zip-top bag) in Figure F8 was collected from that location. The projected model forecast for the 15 October episode is presented in Figure F9, and Figures F3 and F4 clearly illustrate the arrival of African dust at our research sites for these two episodes.

Particle count data and the strength of correlations with surface water communities and atmospheric communities will be evaluated again after chemical analyses of the high-volume filters. This evaluation is necessary to verify sources and to determine if the light gray to dark gray filters are an artifact of diesel exhaust or particulates from biomass burning in Europe or Africa. These data along with those such as wind speed, wind direction, and ship orientation will be valuable in determining which air masses and their sources influenced these communities. As an example, if the illustrated peak in atmospheric particulate matter that occurred on 8–10 October is removed (this was a period of low wind speed, where ship exhaust was contributing to particulate counts, as illustrated in Figs. F1 [low wind condition] and F3 [graying of the filter material]), then the correlation between total CFU and particle counts in the low-volume B samples strengthens from an *r* value of 0.360–0.410 and a *P* value of 0.017–0.008. (shift from a weak to a moderate strength correlation). Obviously, additional shore-based data and a more careful interpretation of the data are needed to accurately evaluate the true extent of the observed relationships outlined in this report and for those yet to be determined.

References

Barrie, L.A., Gregor, D., Hargrave, B., Lake, R., Muir, D., Shearer, R., Tracey, B., and Bidleman, T., 1992. Arctic contaminants: sources, occurrence, and pathways. *Sci. Total Environ.*, 122(1–2):1–74. doi:10.1016/0048-9697(92)90245-N

Chen, P.-S., Tsai, F.T., Lin, C.K., Yang, C.-Y., Chan, C.-C., Young, C.-Y., and Lee, C.-H., 2010. Ambient influenza and avian influenza virus during dust storm days and background days. *Environ. Health Perspect.,* 118(9):1211–1216. doi:10.1289/ehp.0901782

Coe, M.T., and Foley, J.A., 2001. Human and natural impacts on the water resources of the Lake Chad basin. *J. Geophys. Res., [Atmospheres],* 106(D4):3349–3356. doi:10.1029/2000JD900587

Criado, C., and Dorta, P., 2003. An unusual "blood rain" over the Canary Islands (Spain). The storm of January 1999. *J. Arid Environ.,* 55(4):765–783. doi:10.1016/S0140-1963(02)00320-8

Garrison, V.H., Foreman, W.T., Genualdi, S., Griffin, D.W., Kellogg, C.A., Majewski, M.S., Mohammed, A., Ramsubhag, A., Shinn, E.A., Simonich, S.L., and Smith, G.W., 2006. Saharan dust—a carrier of persistent organic pollutants, metals, and microbes to the Caribbean? *Rev. Biol. Trop.,* 54(Suppl. 3):9–21. http://www.scielo.sa.cr/pdf/rbt/v54s3/3389.pdf

Gillies, J.A., Nickling, W.G., and Mctainsh, G.H., 1996. Dust concentrations and particle-size characteristics of an intense dust haze event: inland delta region, Mali, West Africa. *Atmos. Environ.,* 30(7):1081–1090. doi:10.1016/1352-2310(95)00432-7

Goudie, A.S., and Middleton, N.J., 2001. Saharan dust storms: nature and consequences. *Earth-Sci. Rev.,* 56(1–4):179–204. doi:10.1016/S0012-8252(01)00067-8

Graham, W.F., and Duce, R.A., 1979. Atmospheric pathways of the phosphorus cycle. *Geochim. Cosmochim. Acta,* 43(8):1195–1208. doi:10.1016/0016-7037(79)90112-1

Griffin, D., Kellogg, C., Garrison, V., and Shinn, E., 2002. The global transport of dust. *Am. Sci.,* 90(3):228–235. doi:10.1511/2002.3.228

Griffin, D.W., 2007. Atmospheric movement of microorganisms in clouds of desert dust and implications for human health. *Clin. Microbiol. Rev.,* 20(3):459–477. doi:10.1128/CMR.00039-06

Griffin, D.W., Garrison, V.H., Herman, J.R., and Shinn, E.A., 2001. African desert dust in the Caribbean atmosphere: microbiology and public health. *Aerobiologia,* 17(3):203–213. doi:10.1023/A:1011868218901

Griffin, D.W., Westphal, D.L., and Gray, M.A., 2006. Airborne microorganisms in the African desert dust corridor over the Mid-Atlantic Ridge, Ocean Drilling Program, Leg 209. *Aerobiologia,* 22(3):211–226. doi:10.1007/s10453-006-9033-z

Grini, A., and Zender, C.S., 2004. Roles of saltation, sandblasting, and wind speed variability on mineral dust aerosol size distribution during the Puerto Rican Dust Experiment (PRIDE). *J. Geophys. Res., [Atmospheres],* 109(D7):D07202. doi:10.1029/2003JD004233

Isard, S.A., and Gage, S.H., 2001. *Flow of Life in the Atmosphere: An Airscape Approach to Understanding Invasive Organisms:* East Lansing, MI (Michigan State Univ. Press).

Jaenicke, R., 2005. Abundance of cellular material and proteins in the atmosphere. *Science,* 308(5718):73. doi:10.1126/science.1106335

Koren, I., Kaufman, Y.J., Washington, R., Todd, M.C., Rudich, Y., Martins, J.V., and Rosenfeld, D., 2006. The Bodélé depression: a single spot in the Sahara that provides most of the mineral dust to the Amazon forest. *Environ. Res. Lett.,* 1(1):014005. doi:10.1088/1748-9326/1/1/014005

Lenes, J.M., Darrow, B.P., Cattrall, C., Heil, C.A., Callahan, M., Vargo, G.A., Byrne, R.H., Prospero, J.M., Bates, D.E., Fanning, K.A., and Walsh, J.J., 2001. Iron fertilization and the *Trichodesmium* response on the West Florida

shelf. *Limnol. Oceanogr.,* 46(6):1261–1277. doi:10.4319/lo.2001.46.6.1261

Middleton, N.J., and Goudie, A.S., 2001. Saharan dust: sources and trajectories. *Trans. Inst. Br. Geogr.,* 26(2):165–181. doi:10.1111/1475-5661.00013

Moulin, C., Lambert, C.E., Dulac, F., and Dayan, U., 1997. Control of atmospheric export of dust from North Africa by the North Atlantic Oscillation. *Nature (London, U. K.),* 387(6634):691–694. doi:10.1038/42679

O'Hara, S.L., Wiggs, G.F.S., Mamedov, B., Davidson, G., and Hubbard, R.B., 2000. Exposure to airborne dust contaminated with pesticide in the Aral Sea region. *Lancet,* 355(9204):627–628. doi:10.1016/S0140-6736(99)04753-4

O'Malley, M.A., and McCurdy, S.A., 1990. Subacute poisoning with phosalone, an organophosphate insecticide. *West. J. Med.,* 153(6):619–624. http://www.ncbi.nlm.nih.gov/pmc/articles/PMC1002638/

Perkins, S., 2001. Dust, the thermostat: how tiny airborne particles manipulate global climate. *Sci. News,* 160(13):200–202. doi:10.2307/4012776

Perry, K.D., Cahill, T.A., Eldred, R.A., Dutcher, D.D., and Gill, T.E., 1997. Long-range transport of North African dust to the eastern United States. *J. Geophys. Res., [Atmospheres],* 102(D10):11225–11238. doi:10.1029/97JD00260

Prospero, J.M., 1999. Long-term measurements of the transport of African mineral dust to the southeastern United States: implications for regional air quality. *J. Geophys. Res., [Atmospheres],* 104(D13):15917–15927. doi:10.1029/1999JD900072

Prospero, J.M., and Lamb, P.J., 2003. African droughts and dust transport to the Caribbean: climate change implications. *Science,* 302(5647):1024–1027. doi:10.1126/science.1089915

Prospero, J.M., and Nees, R.T., 1986. Impact of the North African drought and El Niño on mineral dust in the Barbados trade winds. *Nature (London, U. K.),* 320(6064):735–738. doi:10.1038/320735a0

Qian, W., Quan, L., and Shi, S., 2002. Variations of the dust storm in China and its climatic control. *J. Clim.,* 15(10):1216–1229. doi:10.1175/1520-0442(2002)015<1216:VOTDSI>2.0.CO;2

Shinn, E.A., Griffin, D.W., and Seba, D.B., 2003. Atmospheric transport of mold spores in clouds of desert dust. *Arch. Environ. Health,* 58(8):498–504. http://www.ncbi.nlm.nih.gov/pubmed/15259429

Tate, R.L., III, 2000. *Soil Microbiology* (2nd ed.): New York (John Wiley and Sons, Inc).

Tucker, C.J., and Nicholson, S.E., 1999. Variations in the size of the Sahara Desert from 1980 to 1997. *Ambio,* 28(7):587–591. http://www.jstor.org/stable/10.2307/4314962

Walsh, J.J., and Steidinger, K.A., 2001. Saharan dust and Florida red tides: the cyanophyte connection. *J. Geophys. Res., [Oceans],* 106(C6):11597–11612. doi:10.1029/1999JC000123

Weir-Brush, J.R., Garrison, V.H., Smith, G.W., and Shinn, E.A., 2004. The relationship between gorgonian coral (Cnidaria: Gorgonacea) diseases and African dust storms. *Aerobiologia,* 20(2):119–126. doi:10.1023/B:AERO.0000032949.14023.3a

Whitman, W.B., Coleman, D.C., and Wiebe, W.J., 1998. Prokaryotes: the unseen majority. *Proc. Natl. Acad. Sci. U. S. A.,* 95(12):6578–6583. doi:10.1073/pnas.95.12.6578
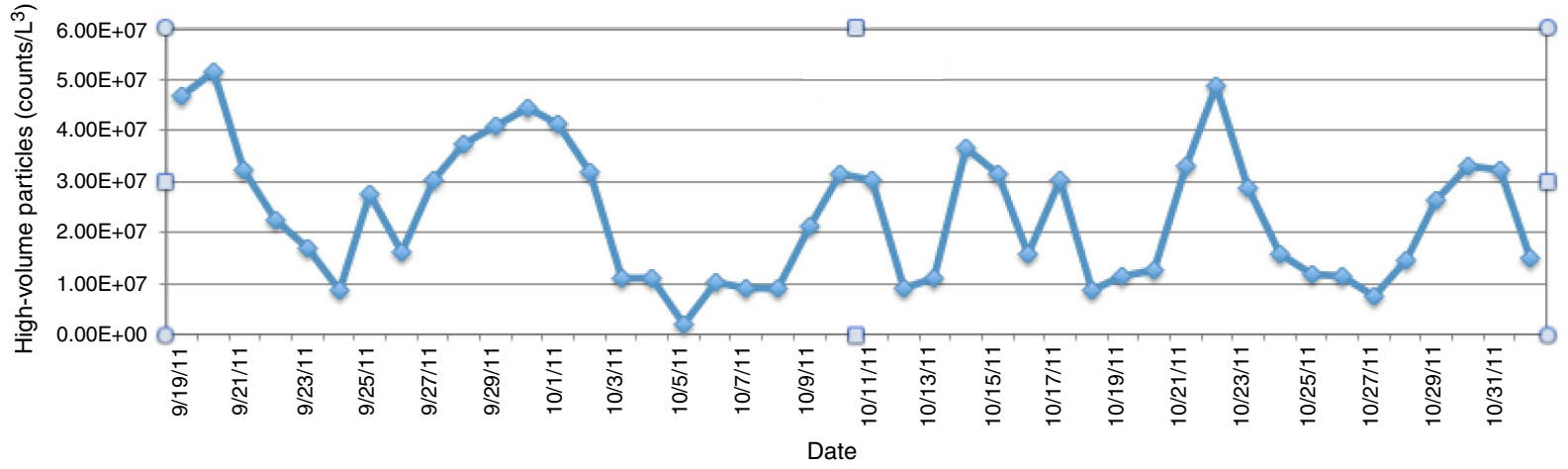
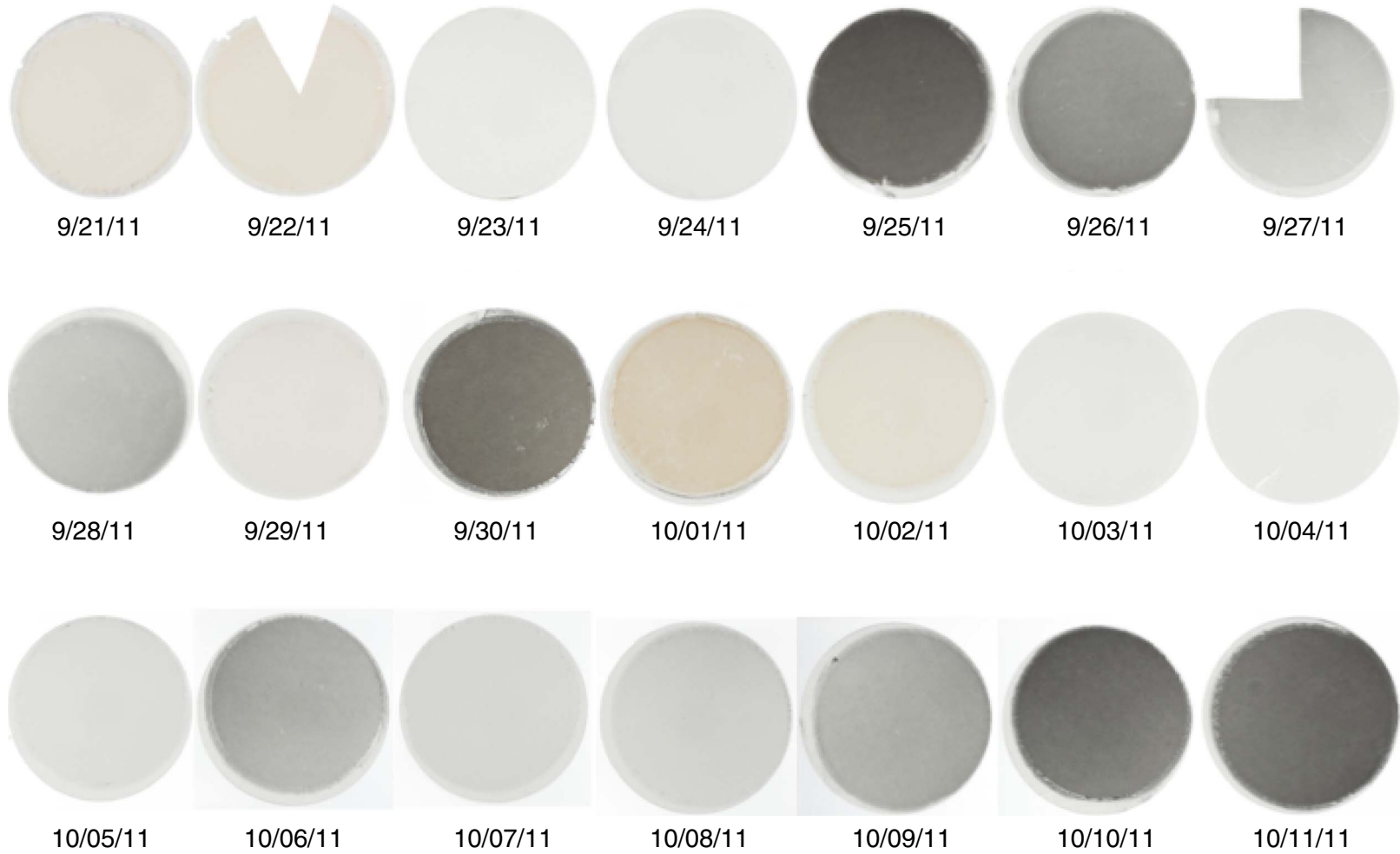**Figure F1.** Daily wind speed in meters per second taken between 0455 and 0710 h EST.
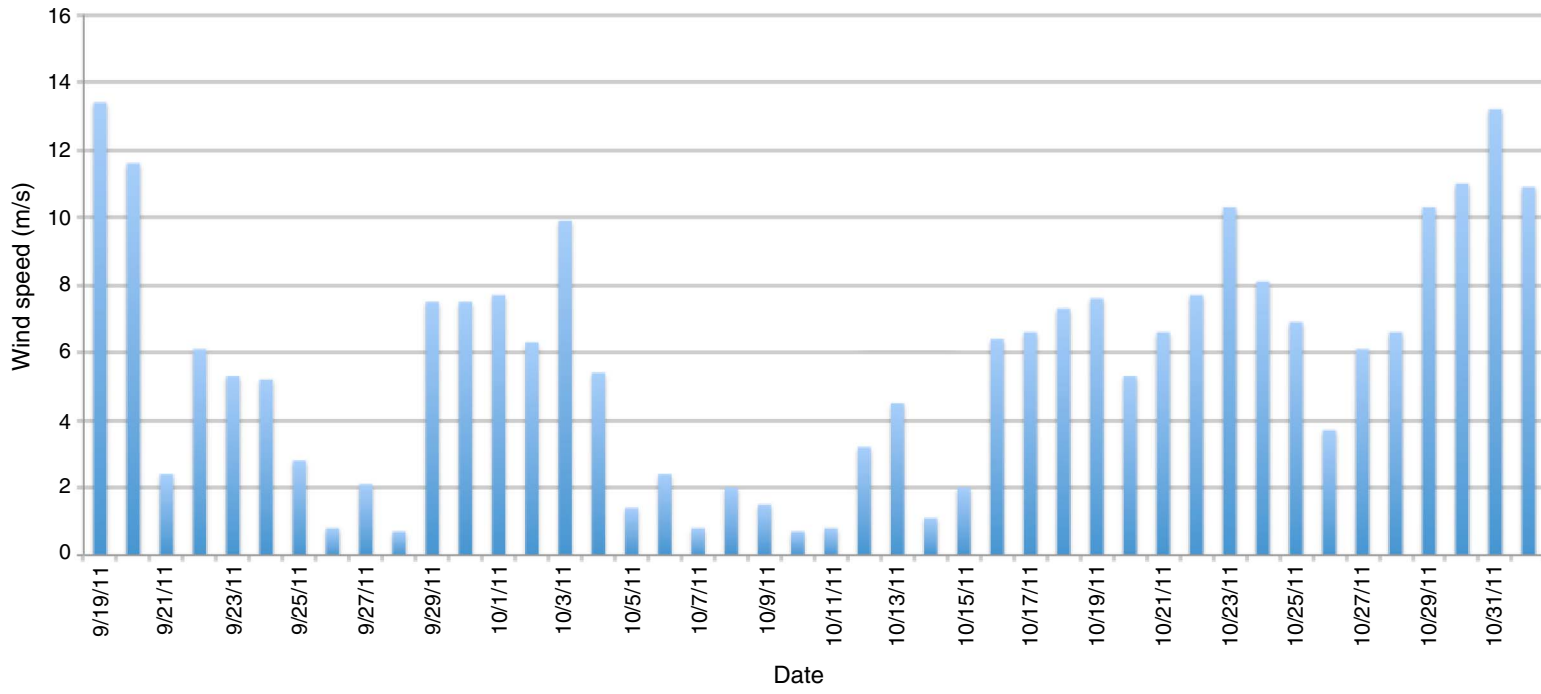
Figure F2. Daily average of particle counts per cubic liter of air for the high-volume sample time period (~24 h; 0645 h to 0715 h EST the following day).

Figure F3. High-volume sample filters collected daily over ~24 h. Filters are Staplex Type TFAGF41 glass fiber filters. Time period is 21 September–11 October 2011.

| 9/21/11 | 9/22/11 | 9/23/11 | 9/24/11 | 9/25/11 | 9/26/11 | 9/27/11 |

| 9/28/11 | 9/29/11 | 9/30/11 | 10/01/11 | 10/02/11 | 10/03/11 | 10/04/11 |

| 10/05/11 | 10/06/11 | 10/07/11 | 10/08/11 | 10/09/11 | 10/10/11 | 10/11/11 |

Figure F4. High-volume sample filters collected daily over ~24 h. Filters are Staplex Type TFAGF41 glass fiber filters. Time period is 12 October–1 November 2011.

10/12/11   10/13/11   10/14/11   10/15/11   10/16/11   10/17/11   10/18/11

10/19/11   10/20/11   10/21/11   10/22/11   10/23/11   10/24/11   10/25/11

10/26/11   10/27/11   10/28/11   10/29/11   10/30/11   10/31/11   11/01/11

Figure F5. Particle counts and total bacterial and fungal colony forming units (CFUs) collected daily between 0500 and 1950 h EST. Blue = total CFUs, red = particle counts per cubic liter of air.
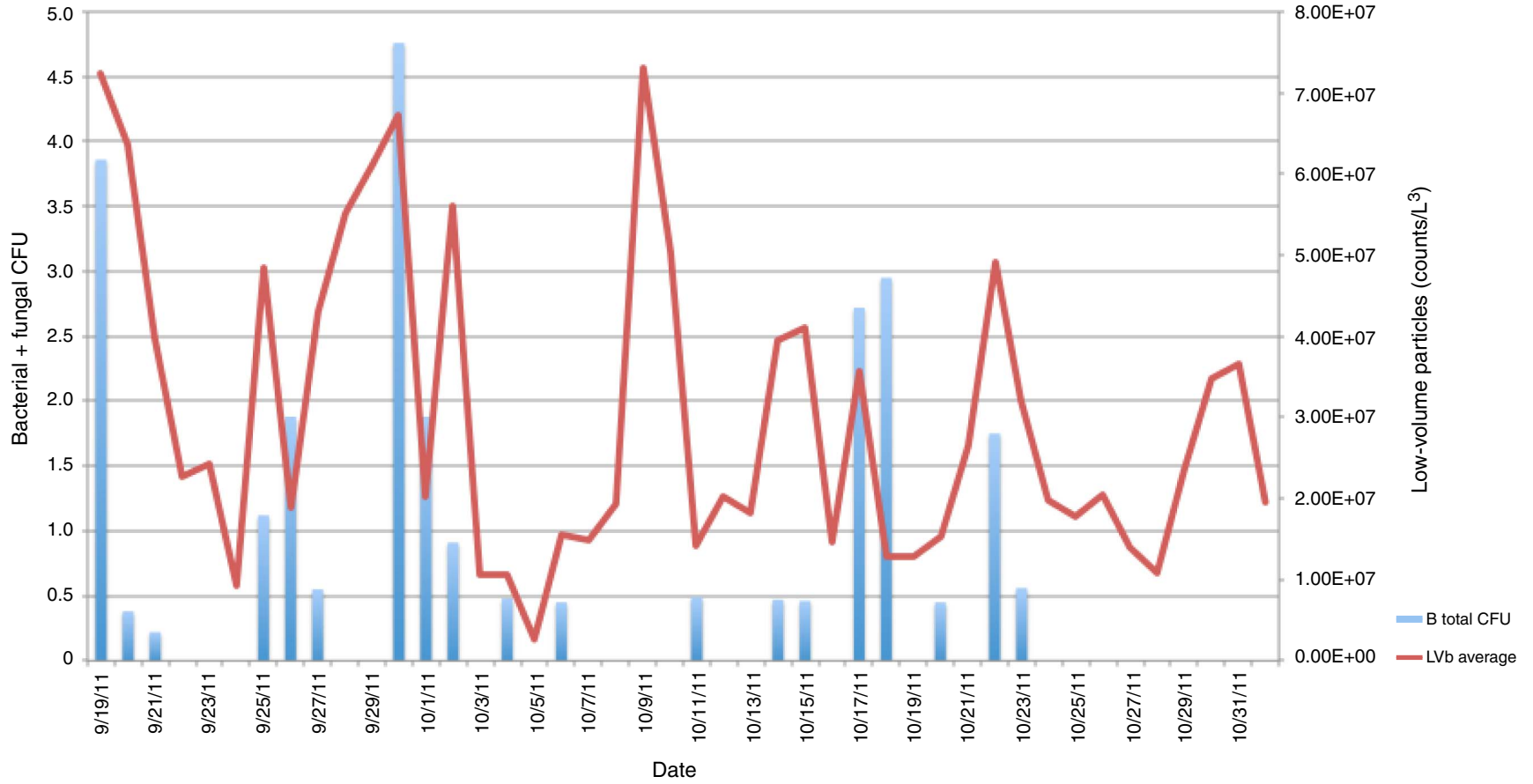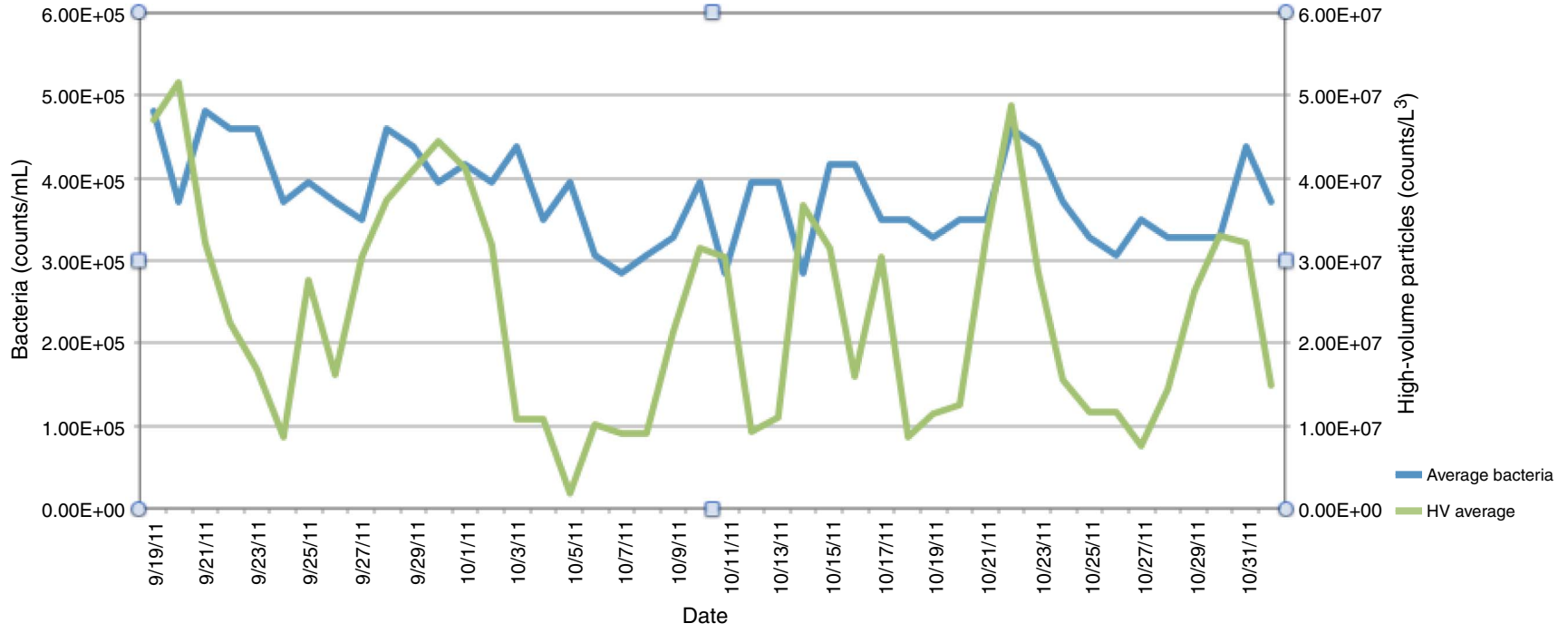
Figure F6. Daily bacterial and viral surface water direct counts (epifluorescent microscopy). Samples were collected between 1100 and 1425 h EST. Counts are bacterial cells and viruslike particles per milliliter of water.
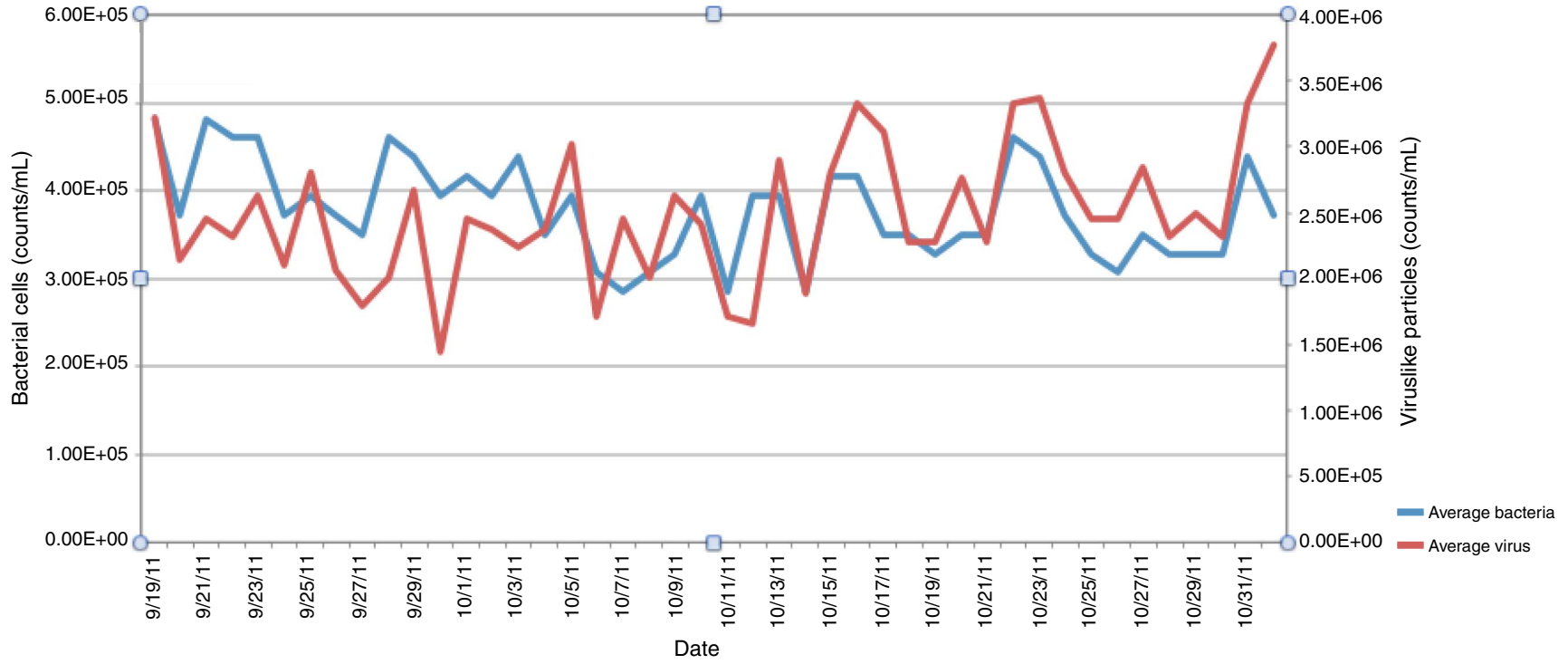
Figure F7. Bacterial direct counts per milliliter of surface water and averaged daily high-volume (HV) particle counts per cubic liter of air.

Figure F8. African dust fall-out collected from the bridge roof of the *JOIDES Resolution* on 6 October 2011. Notice the fine nature of the dust clinging to the inner surface of the bag. The larger deposits at the top of the photograph are the result of collection in damp conditions and subsequent open drying in a fume hood.
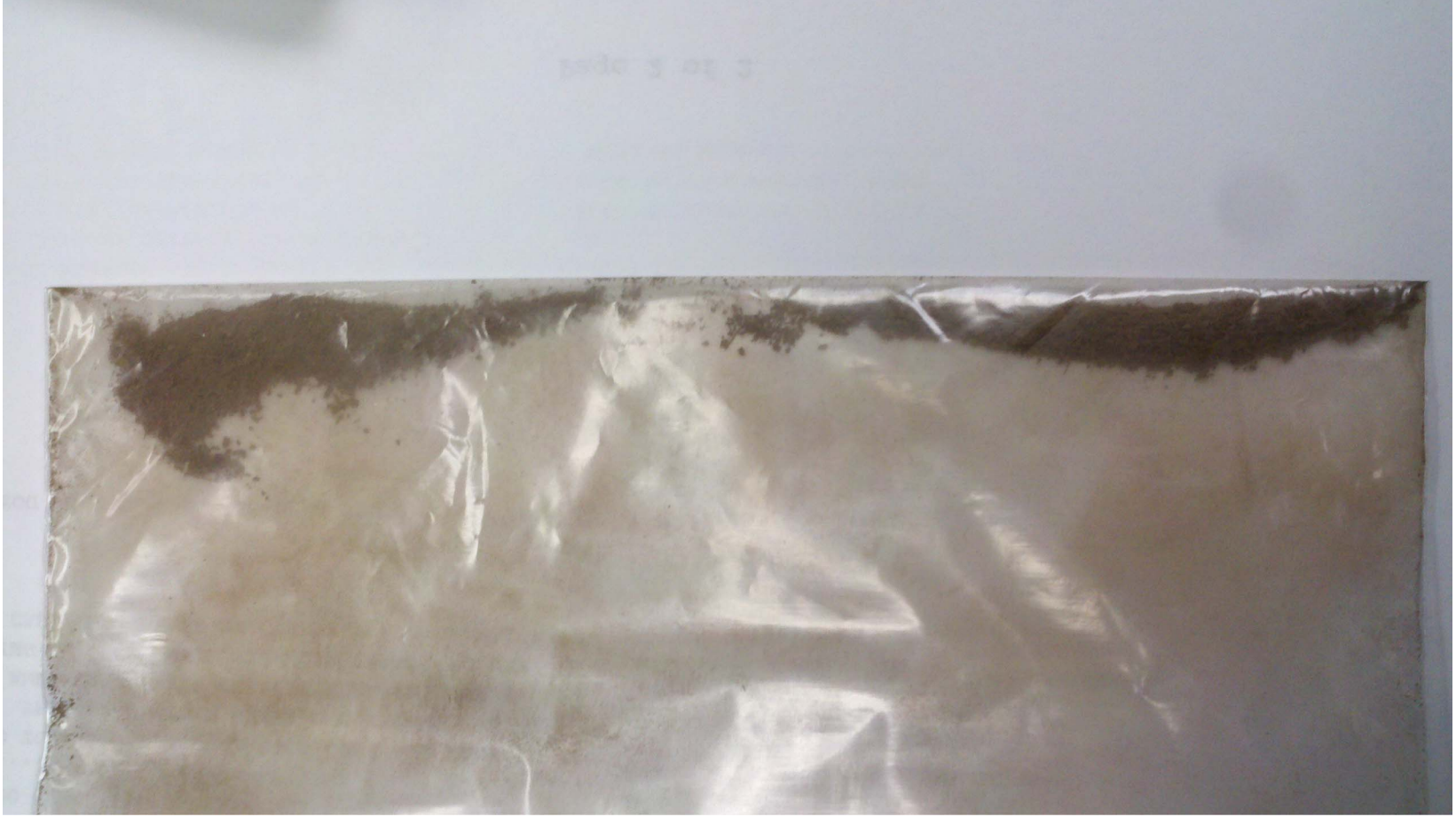
Figure F9. Model forecast of African desert dust impacting Expedition 336 drill sites on 15 October 2011. Model image courtesy of Cristina Gonzalez, University of La Laguna, Canary Islands.